Tropical Plant Pathology (2022) 47:152–167
https://doi.org/10.1007/s40858-021-00460-2

ORIGINAL ARTICLE

Identification of diseases and physiological disorders in potato via multispectral drone imagery using machine learning tools

William A. León-Rueda[1] · Camilo León[2] · Sandra Gómez- Caro[1] · Joaquín Guillermo Ramírez-Gil[1]

Received: 23 November 2020 / Accepted: 22 July 2021 / Published online: 20 September 2021

Abstract

The rapid and precise detection of diseases and plant disorders is the basis for the adequate and timely design of management strategies. Currently, there are several non-destructive alternatives that allow early detection, highlighting the use of spectral cameras attached to unmanned aerial vehicles (UAVs). The objective of this research was to evaluate the use of multispectral cameras on UAVs to discriminate vascular wilt caused by *Verticillium* spp., (VW), waterlogging stress (WL), and an unknown alteration (UA) in commercial potato (*Solanum tuberosum*) variety "Diacol Capiro" crops. Plots were monitored during the crop cycle, performing the visual characterization of the diseases and disorders present. Five spectral band images were acquired using a MicaSense RedEdge spectral camera attached to a Map-T680 hexacopter drone to extract the bands and calculate the vegetation indices that were calibrated and evaluated to determine their ability to discriminate between diseased and healthy plants based on a generalized linear model (GLM) and Kappa index. Additionally, the supervised random forest classification method was implemented, optimized, and evaluated using the accuracy, area under receiver operating characteristic curve (ROC-AUC), kappa index, and inference error based on k-fold cross-validation. After algorithms optimization our results show a classifier accuracy, kappa and ROC-AUC values to VW, WL and UA between 73.5–82.5%, 0.56–0.71, 0.97–0.98, and 35 37.5–51.9%, 0.07–0.06, and 0.88–0.94 for plots 1 and 2, respectively. This study reports an approach to the use of multispectral cameras attached to UAVs as a tool with potential for the detection of diseases and physiological disorders in commercial potato crops.

Keywords Vegetation indices · Model calibration · Early detection · Data science

Introduction

The potato (*Solanum tuberosum* L.) crop is affected by multiple phytosanitary problems that may vary according to the biogeographic regions where it is planted. Late blight (LB) caused by *Phytophthora infestans* (Mont.) de Bary has been reported as the most destructive disease with the greatest potential for damage (Fry et al. 1993; Ristaino 2002). However, vascular wilt (VW) or early dying caused by *Verticillium* is a phytosanitary problem of increasing importance in this crop, with *Verticillium dahliae* Kleb. and *Verticillium albo-atrum* Reinke & Berthold as the main reported species (Krikun and Orion 1979; Johnson and Dung 2010; Wheeler and Johnson 2016).

In Colombia, LB is considered the most important disease (Silva et al. 2010; Céspedes et al. 2013); *Verticillium* has been reported in the departments of Antioquia, Boyacá, Nariño, Norte de Santander, and Cundinamarca (Nieto 1988; Buriticá-Cespedes 1999), with important economic and epidemiological implications in the last few years (Ramirez-Gil et al. 2019a). Additionally, an alteration has been observed in recent crop cycles. This alteration differs from the disorders or diseases previously reported in potato crops (Stevenson et al. 2002; Torres 2002), because of its symptoms and development

✉ Joaquín Guillermo Ramírez-Gil
jgramireg@unal.edu.co

[1] Departamento de Agronomía, Facultad de Ciencias Agrarias, Universidad Nacional de Colombia Sede Bogotá, Bogotá, D.C, Colombia

[2] 3D Geoinformation Group, Delft University of Technology, Julianalaan 134, 2628BL Delft, Netherlands

in affected plants. In this study, it is called unknown alteration (UA) and has negatively affected crop yields and production quality (Ramirez-Gil et al. 2019b). Mayor symptoms of UA are associated with a reduction of the stem rigidity, yellowing of the lower leaves in late stages, and early plant maturity (Ramirez-Gil et al. 2019b). Based on the literature reviewed and field and laboratory tests carried out by our research group, it has not been possible to relate UA to a specific causal agent or to an abiotic factor; for these reasons, further studies are needed to clarify the etiology of these symptoms. This problem has been observed in production areas in the municipalities of Madrid and Mosquera in Cundinamarca, Guatavita in Boyacá, and Cajamarca in the department of Tolima (Ramirez-Gil et al. 2019b). On the other hand, the water excess or waterlogging (WL) in the soil has been reported as a consequence of the ENSO phenomena (especially La Niña). Water stress has recently increased in the country, affecting different crops and causing plant disorders (Ramírez-Gil and Morales-Osorio 2018).

The basis for proper plant disease management must start from early detection in the crop (Miller et al. 2009). The development of biotic or abiotic stress conditions triggers physiological alterations or biochemical changes in plants that can be detected by different types of sensors (Oerke et al. 2006; Fang and Ramasamy 2015; Mahlein et al. 2017; Lowe et al. 2017). In recent years, early detection techniques for disease-causing agents have been introduced through the use of sensors (Mahlein et al. 2018), highlighting the utilization of hyperspectral cameras (Martinelli et al. 2015; Fang and Ramasamy 2015; Mahlein et al. 2017, 2018). The use of these devices has been reported in potato production systems for the detection of potato Y virus (PYV) (Couture et al. 2018; Polder et al. 2019) and late blight (Duarte-Carvajalino et al. 2018). Additionally multispectral cameras on-board unmanned aerial vehicles (UAVs) and multiple types of data measurement and analysis techniques have introduced a novel approach for the rapid and accurate assessment of crop disease level. In potato, incidence and early severity levels of diseases such as late blight (Franceschini et al. 2019) and blackleg (*Pectobacterium atrosepticum*) (Gibson-Poole et al. 2017) have been measured using this novel approach.

The identification and diagnosis of plant diseases are especially important in climate change scenarios, in particular for areas with high climatic variability such as Colombia (Ramírez-Gil and Morales-Osorio 2018), and production systems extremely sensitive to different kinds of abiotic and biotic factors like the potato crop. Therefore, early detection and timely management are decisive in reducing the losses that these factors may cause. The objective of this study was to evaluate the use of multispectral cameras attached to UAVs and image processing using a machine learning tool for the discrimination of diseases and plant disorders (VW, WL, and UA) in commercial potato crops.

Materials and methods

Location, sampling, characterization of diseases, and description of physiological disorders present in the potato crop

We evaluated two commercial potato plots of the variety "Diacol Capiro" and located in the municipality of Subachoque (Cundinamarca, Colombia): Plot 1 (4.9685931, -74.1545059, 2754 m) of 8 ha with high topographic variation, so the field was divided into three areas depending on the slope (in percentage) ((i) < 5%, (ii) 5.1–10%, and (iii) > 10%, with 45, 30 and 25% of area, respectively) and Plot 2 (4.959364175, -74.16033033, 2732 m) of 10 ha with little topographic variation (< 5% slope).

Based on previous temporal dynamics analysis in the appearing of symptoms (incubation period reported) of VW disease (> 70 days after sowing (das)) and UA disorder (> 60 das) and when the level of incidence and disease severity were high enough for visual discrimination, plots 1 and 2 were monitored at 90–120 and 75–105 das, respectively. The number sample points are calculated according to the maximum variance formula (Eq. 1) (Cochran 1977). A sampling unit of 2 m^2 (approximately 5 plants) was considered, with 90 (plot 1) and 106 (plot 2) points distributed in the space using a proportional stratified sampling (% of area-slope category) for plot 1 and simple random sampling for plot 2. The number of samples was determined as a relationship between the flexibility under field sampling for decision making, the maximum margin of error (20%), and the confidence level (80%) allowed to achieve population inference.

In each plot, presence-absence evaluations to calculate the disease incidence (number of symptomatic plants over the total evaluated plants) were conducted. Additionally, for all alterations and diseases under study, visual severity

scoring using a four level scale was evaluated at each point (no disease = 0; slight disease = 1 (leaf area affected between 0.1 and 20%); moderate disease = 2 (leaf area affected between 20.1 and 50%); and high disease level = 3 (leaf area affected > 50.1%)), and their respective coordinates were collected.

$$n = \frac{Z^2P(1-P)/e^2}{1+(Z^2P(1-P)/e^2N}, \quad (1)$$

where n is the sample size; N is the population size; e is the error margin (20%); z is the value based on confidence level (80% = 1.28); and P is the probability (0.5%).

Before recording the incidence, severity, and spatial location of the points to be sampled, a pre-sampling was carried out to describe the symptoms associated with each case and their importance. This pre-sampling was based on a field-farms monitoring approach following a random sampling with a "n" of 80 and 75 points for plots 1 and 2, respectively. VW, LB, WL, and UA were selected according to their incidence in the plots under study. Additionally, samples of symptomatic and asymptomatic plants were collected in each plot. The samples were taken to the Plant Clinic of the Faculty of Agricultural Sciences at the Universidad Nacional de Colombia for processing and identification of the associated causal agents.

In the laboratory, pathogens were isolated from the base of stems, roots, and leaves of the plants to be analyzed. For this purpose, plant tissue was cut and disinfected with 70% ethanol for 30 s and 2% NaOCl for 30 s followed by two washes in sterile distilled water and cultured in Petri dishes with Potato Dextrose Agar (PDA) (Oxoid®) medium acidified to 0.1% (v/v) with 85% lactic acid. Petri dishes were incubated in the dark at 25 °C for 10 days, and the frequency of fungal and bacterial colonies was recorded. The isolated fungi were morphologically identified at the genus level following a taxonomic key (Barnett and Hunter 1972; Seifert et al. 2011), and the same procedure was carried out for oomycete species (Erwin and Ribeiro 1996).

Multispectral image capture using a camera attached to a UAV

Based on the monitoring in previous sampling procedures, stable environmental parameters for the appropriate flight and spectral capture planning (e.g., flight altitude, image overlap, flying direction, flying speed, solar elevation, cloudiness, and wind speed) (Tu et al. 2020) and availability of the equipment were adjusted to the second sampling (120 and 105 das for plots 1 and 2, respectively).

Multispectral data was captured in each plot using the MicaSense RedEdge multispectral sensor (MicaSense®), with a DLS 2 type light sensor (Downwelling Light Sensor, MicaSense®) for correcting mid-flight lighting changes, ground control points (GCP) for geometric correction, and a reflectance panel (MicaSense®) for radiometric correction of images. The sensor was attached to a hexacopter-type UAV Map-T680 following a flight plan 120 m above the ground, with an 80% overlap between images and a 60% overlap between flight lines. Images were captured with a pixel size of 8 cm in the spectral bands blue (475-nm center, 20-nm bandwidth), green (560-nm center, 20-nm bandwidth), red (668-nm center, 10-nm bandwidth), red edge (717-nm center, 10-nm bandwidth), and near infrared (NIR) (840-nm center, 40-nm bandwidth). Agisoft Metashape 1.6.1 (Agisoft™) was used for the post-processing of data and the generation of orthophotomosaics.

Evaluation of diseases and disorders discrimination capacity using vegetation indices

Different vegetation indices reported for the detection of plant alterations were calculated from the processed orthophotomosaics (Table 1). These products were then projected to the evaluated plots. This process was carried out using the LSRS package for R (Sarparast 2018).

Table 1 Vegetation indices used for disease plants detection and the mathematical expressions to calculate them

Name	Estimation	Reference
Normalized difference vegetation index (NDVI)	$^{R}_{NIR}\text{-}^{R}_{RED}/R_{NIR}+{}^{R}_{RED}$	Naidu et al. (2009)
Soil-adjusted vegetation index (SAVI)	$(^{R}_{NIR}\text{-}^{R}_{RED})\ (1+L)/{}^{R}_{NIR}+{}^{R}_{RED}+{}^{La}$	Yang et al. (2007)
Modified soil-adjusted vegetation index (MSAVI)	$(^{R}_{NIR}\text{-}^{R}_{RED})\ (1+L)/{}^{R}_{NIR}+{}^{R}_{RED}+{}^{Lb}$	Qi et al. (1994)
Enhanced vegetation index (EVI)	$G^{*}\ ((^{R}_{NIR}\text{-}^{R}_{RED})/(R_{NIR}+C1*{}^{R}_{RED\text{-}}+1))^{c}$	Mondal (2011)
Green normalized difference vegetation index (GNDVI)	$^{R}_{GREEN}\text{-}^{R}_{RED}/{}^{R}_{GREEN}+{}^{R}_{RED}$	Yang et al. (2007)
Visible atmospherically resistance index (VARI)	$^{R}_{GREEN}\text{-}^{R}_{RED}/{}^{R}_{GREEN}+{}^{R}_{RED\text{-}}\ {}^{R}_{BLUE}$	Naidu et al. (2009)

[a]Soil brightness correction factor = 0.5. [b]MSAVI uses the following formula to calculate L, L = 1 − 2 *s *$(^{R}_{NIR}\text{-}^{R}_{RED})$ *$(^{R}_{NIR}\text{-}\ s*{}^{R}_{RED})$/ $(^{R}_{NIR}\text{-}{}^{R}_{RED})$, where s is the slope of the soil line from a plot of red versus near infrared brightness values. [c]G constant = 2.5; C atmospheric resistance coefficients (C1 = 2.4); L to adjust the background = 1

The values for each index were extracted at each sampling point to assess whether the vegetation indices had discriminative capacity between diseased and healthy plants. We opted for a generalized linear model (GLM) using the logarithm of the mean for the link function in the log-linear model. This model was selected to evaluate the discriminative ability considering that the response variable was adjusted to a Poisson distribution (healthy and diseased plants) and the predictive variables were discretized vegetation indices. The potential of each vegetation index for the predictive capacity of the model was evaluated by the root mean square error of prediction (RMSEP) criterion using leave one out cross-validation. As a complement, we used the kappa statistic or coefficient to determine hard classification outputs (healthy vs. diseased), defining four discrimination categories based on their value: (i) perfect (1); (ii) good (0.6–0.99); (iii) moderate (0.3–0.59), and (iv) poor (≤ 0.3) (Viera and Garrett 2005). This procedure was executed in R (R Development Core Team 2020).

Supervised classification of images

We used the random forest (RF) classifier for the classification process (Pal, 2005). The diseases and physiological disorders (VW, WL, and UA), healthy plants (HP), water (W), and soil (S) were used as input classes. The spectral bands obtained by the multispectral camera as well as the calculated vegetation indices reported in Table 1 were used as the predictors. For this analysis, LB was discarded due to its low incidence and severity in the studied plots (incidence and severity less than 5 and 1%, respectively). A number of classes evaluated under field conditions in each plot (1 and 2) were as follows: VW, 25–15; WL, 15–15; UA, 12–20; HP, 45–50; W, 10–10; S, 22–20.

Different variations of input data and parameters were performed within the RF algorithm, by combining variables (bands and bands + indices) and classes: all (VW, WL, UA, HP, W, and S) and reduced (VW, UA, HP, W, and S). The optimization of the RF algorithm as a balance between the robustness, stabilization of the error rate, and computational performance was carried out through a multistep process (Henao-Rojas et al. 2021): (i) evaluating the number of trees (set of combinations from 1 to 1000), (ii) number and depth of nodes (1 to 4000), and (iii) the hyperparameter alpha (0 to 20). In addition, the type of assembly model used in the RF algorithm was bootstrap aggregation technique (Bagging) (Breiman 1996). The arrays data were randomly divided into two data sets: (i) training (75%) and (ii) testing (25%).

Classification on training/validation date set were evaluated following multistep criteria: (i) multiclass-AUC using area under receiver operating characteristic curve (ROC-AUC), related as a measure of the quality of the classification (Cortes and Mohri 2003); (ii) the Kappa index; (iii) inference error using stratified tenfold cross-validation (1—inference error = accuracy); and (iv) significance ($p < 0.05$). In addition to the training process, the confusion matrix (Bekkar et al. 2013; Mueller and Guido 2016) was calculated to evaluate the quality of the classifier, where rows corresponded to the true classes and columns to the predicted classes. From each matrix, the overall accuracy (OA) was calculated using the ratio of the total number of correct samples over the total number of samples (Hasmadi et al. 2009). The classes evaluated were imbalanced, so we changed the prediction rule to other than majority votes (Liaw and Wiener 2002) incorporating artificial class weights into the RF classifier.

The supervised classification and evaluation of the results were carried out by building our code in the free software R, using the following packages: caret (Kuhn et al. 2020) to create folds, fit training, training, and confusion matrix; car (Fox et al. 2020) to test prediction; pROC (Robin et al. 2021) to make the ROC-AUC curves; random forest (Liaw and Wiener 2018) to run the model; randomForestExplainer (Paluszynska et al. 2019) to optimize the RF model; and raster (Hijman 2016) to manipulate spatial data.

Results

Description of the most important diseases and physiological disorders in the evaluated plots

The UA showed the highest incidence (> 30%) and severity (> 10% of leaf area affected) in both plots. Symptoms at early stages were associated with exposure of the abaxial surface of leaves, followed by torsion of leaf petioles and plant stems. Subsequently, chlorosis, death of leaves and branches, and wilted stems on the ground were observed (Fig. 1 A, B, and C). The affected plants did not show visible vascular damage in stems or tubers. At the laboratory, it was not possible to consistently isolate any microorganism

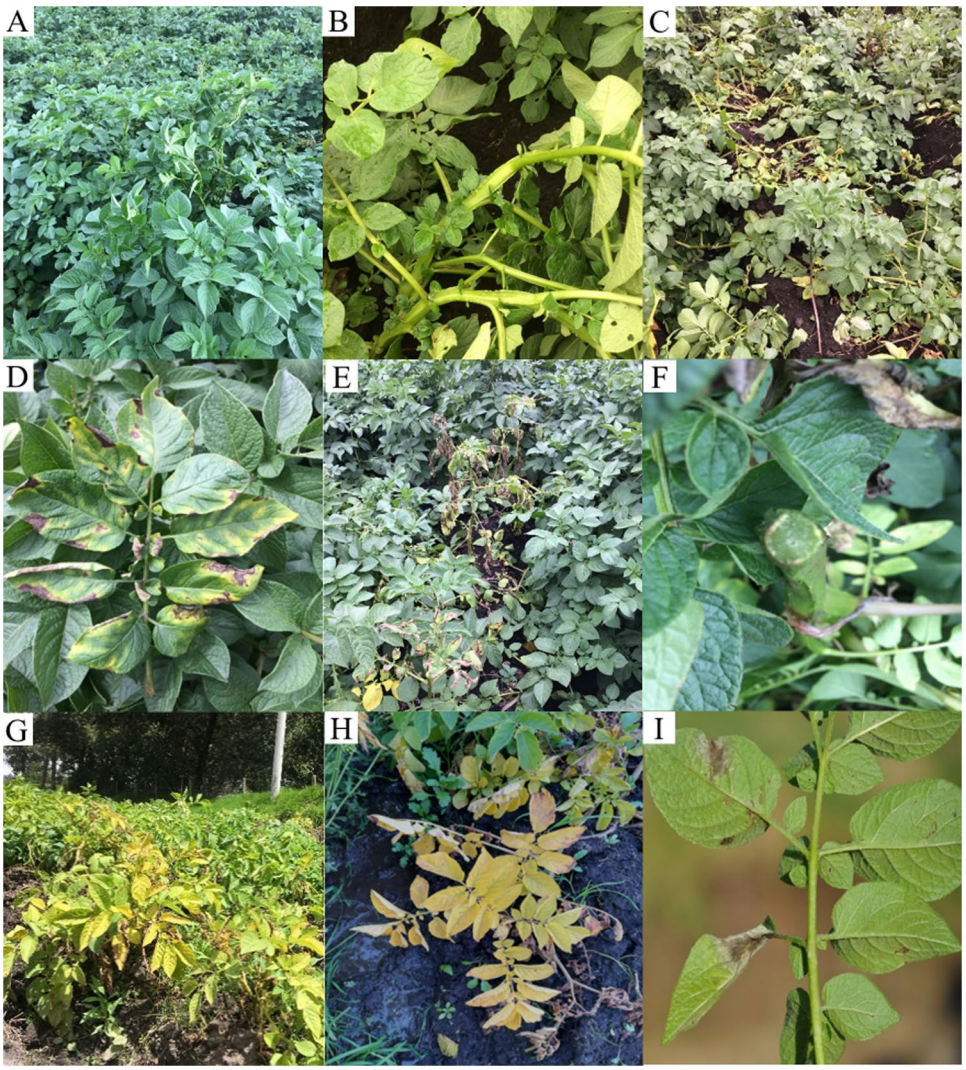

Fig. 1 Diseases and physiological disorders identified in potato plants of the variety Diacol Capiro in commercial plots of the municipality of Subachoque, Cundinamarca, Colombia. **A–C** UA, unknown alteration. **D,E** VW, *Verticillium* Wilt. **G,H** *WL* waterlogging disorder. I: late blight caused by *Phytophthora infestans*

that could be related to this alteration from the evaluated samples.

The second most important disease (VW) showed an incidence greater than 25.6–10.5% and severity values > 10 and < 10% of leaf area affected, in plots 1 and 2, respectively. Symptoms appeared in plants over 30 das and were associated with a hyponastic response, marginal necrosis, interveinal chlorotic areas that advanced towards the main rib, loss of turgidity in stems, unilateral death of branches, and brown coloration in vascular bundles that was evident in cross-sections of the stems (Fig. 1 D, E, and F). From these tissues, it was possible to isolate white, slow-growing cottony colonies in the laboratory. Microscopically, the isolated fungus showed thin, septate, hyaline mycelium that formed single-celled conidia on long conidiophores in whorls and microsclerotia on the hyphae at the edge of the colony, which corresponded to a fungus of the genus *Verticillium* (Barnett and Hunter 1972; Seifert et al. 2011).

The third disorder in importance (WL) showed incidence < 10% and severity < 10% of leaf area affected especially in plot 1. The observed symptoms corresponded to

Table 2 Discrimination capacity of potato diseases and physiological disorders using vegetation indices

Vegetation indices	Disease/ disorder	Statistical test			
		GLM		Kappa index	
NDVI	UA	0.002[a]	12.4[b]	0.65[c]	Good[d]
	VW	0.045	15.8	0.42	Moderate
	LB	0.8	92.3	0.1	Poor
	WL	0.055	132.4	0.2	Poor
SAVI	UA	0.045	35.4	0.42	Moderate
	VW	0.049	63.4	0.31	Moderate
	LB	0.9	122.4	0.09	Poor
	WL	0.065	172.3	0.12	Poor
MSAVI	UA	0.047	40.3	0.45	Moderate
	VW	0.048	58.9	0.39	Moderate
	LB	0.89	104.8	0.1	Poor
	WL	0.060	95.4	0.17	Poor
EVI	UA	0.039	25.3	0.42	Moderate
	VW	0.04	50.3	0.31	Moderate
	LB	0.75	112.4	0.09	Poor
	WL	0.072	165.7	0.09	Poor
GNDVI	UA	0.001	10.3	0.7	Good
	VW	0.0035	12.3	0.6	Good
	LB	0.66	105.8	0.18	Poor
	WL	0.065	132.4	0.19	Poor
VARI	UA	0.038	42.8	0.5	Moderate
	VW	0.045	68.3	0.42	Moderate
	LB	0.93	155.2	0.007	Poor
	WL	0.059	97.3	0.11	Poor

NDVI normalized difference vegetation index, *SAVI* soil-adjusted vegetation index, *MSAVI* modified soil-adjusted vegetation index, *EVI2* enhanced vegetation index, *GNDVI* green normalized difference vegetation index, *VARI* visible atmospherically resistance index, *GLM* generalized lineal model. [a]Significance 0, 0.001, 0.01, and 0 .05. [b]*RMSEP* root mean square error of prediction. [c]Kappa index. [d]Descriptive classifier according to kappa index. *UA* unknown alteration, *VW Verticillium* wilt, *LB* late blight caused by *Phytophthora infestans*, *WL* waterlogging disorder

Table 3 Optimized parameters and statistics metrics of random forest machine learning method to ability for discrimination of classes of diseases and physiological disorders in potato plants of the variety Diacol Capiro

Plot	Model	Optimized parameters in the random forest algorithm				Statistical metrics in training/testing data set							
		mtry[1]	Mean number of nodes	Mean minimum depth	Hyperparameter alpha	Accuracy[2]		Kappa		Multiclass-AUC[3]		*p* Value[4]	
1	Bands—all class	5	728	1.79	4	0.82[a]	0.92[b]	0.71[a]	0.90[b]	0.97[a]	0.98[b]	***[a]	***[b]
	Bands + index—all class	6	320.4	2.72	5	0.73	0.92	0.56	0.90	0.96	0.98	***	***
	Bands + index—selected class	11	362.7	2.33	6	0.79	0.90	0.62	0.87	0.97	0.97	***	***
2	Bands—all class	3	1116.2	1.97	3	0.37	0.72	0.04	0.65	0.92	0.94	*	**
	Bands + index—all class	11	425.1	3.27	4	0.25	0.72	0.06	0.65	0.95	0.96	*	**
	Bands + index—selected class	11	480.5	2.90	5	0.35	0.66	0.07	0.53	0.87	0.88	*	**

[1]Number of variables available for splitting at each tree node (square root of the number of predictor variables). [2]Inference error using stratified tenfold cross-validation (1—inference error = accuracy). [3]Determined parameter using area under receiver operating characteristic (ROC) curve (AUC). [4]Significance codes: ***0001; **0.01; *0.05. [a]Training data set. [b]Testing data set

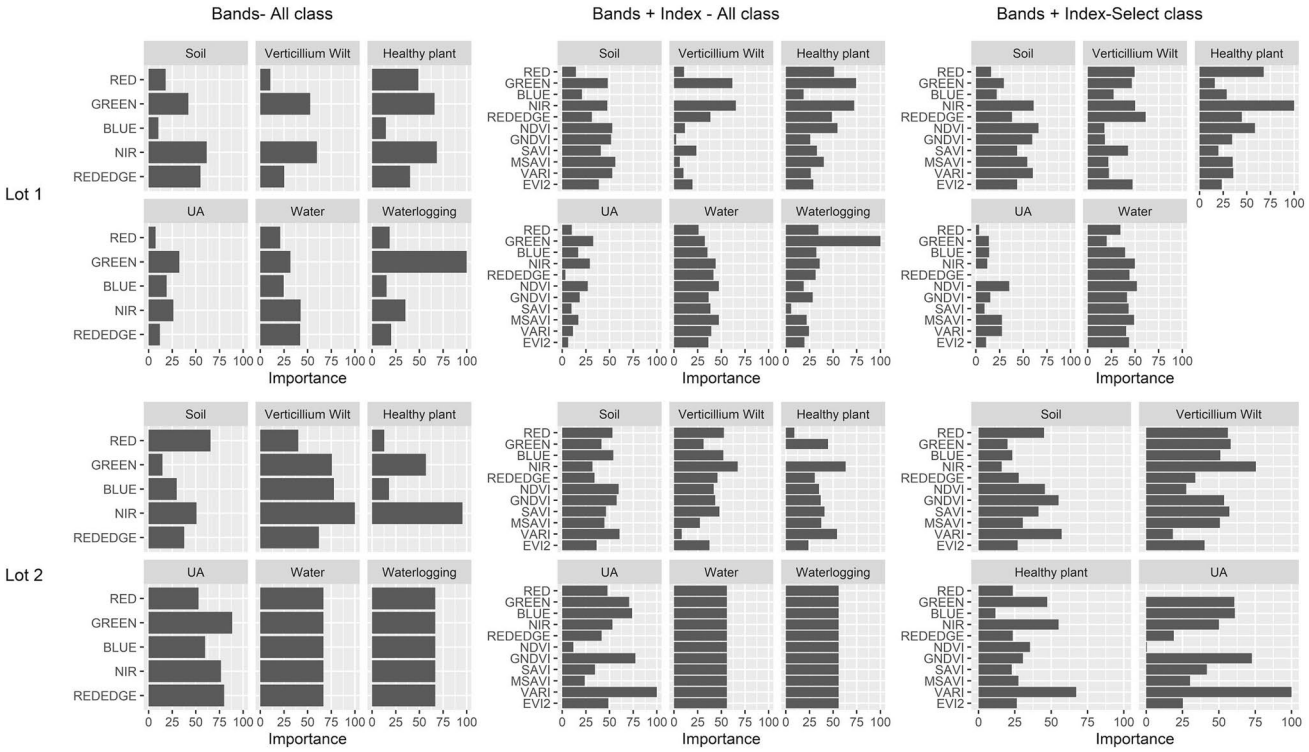

Fig. 2 Importance of variables on the discrimination of classes of diseases and physiological disorders in potato plants of the variety Diacol Capiro using the random forest algorithm. UA: unknown alteration

plants with little shoot and root development, with generalized chlorosis that ended up with the death of the plant at advanced stages (Fig. 1 G and H). These symptoms were associated with waterlogged areas in the plots. No fungal colonies or plant pathogenic bacteria were isolated from plants that displayed these alterations.

`The fourth disease (LB), with an incidence and a leaf area affected less than 5 and 1% respectively in both plots, was associated with irregular necrotic spots on leaves, which initially showed an oily appearance and then invaded a significant portion of the tissue. The microscopic characteristics of the pathogen isolated from infected plant tissue corresponded to *P. infestans* (Erwin and Ribeiro 1996) (Fig. 1H).

Ability to discriminate potato diseases and physiological disorders using vegetation indices

It was found at p value and RMSEP statistics that all the evaluated indices could discriminate diseased plants with over 10% of the leaf area affected (severity) associated with UA and VW, but not for LB and WL, for which the affected area was lower than 10%. This result was confirmed by the kappa index, where qualitative classification yielded parameters of good and moderate discrimination capacity of plants affected by UA and VW (Table 2). Within each index, there were differences in their ability to discriminate healthy

A

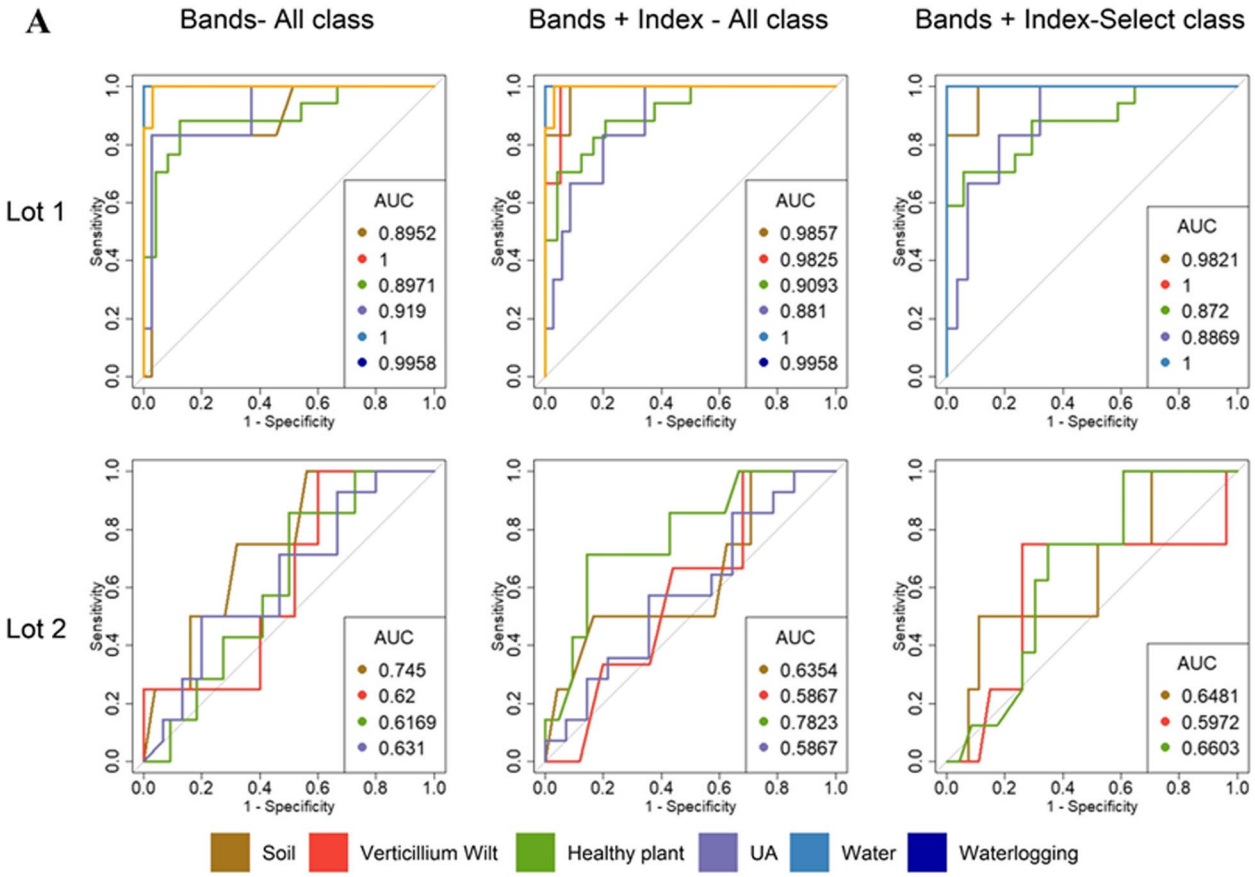

B

Lot 1

Bands- All class

	S	VW	HP	UA	W	WL
S	2	0	0	0	0	0
VW	0	2	0	0	0	0
HP	0	0	4	0	0	0
UA	0	0	1	1	0	0
W	0	0	0	0	1	0
WL	0	0	0	0	0	2

Accuracy 0.923

Bands + Index - All class

	S	VW	HP	UA	W	WL
S	2	0	0	0	0	0
VW	0	2	0	0	0	0
HP	0	0	4	0	0	0
UA	0	0	1	1	0	0
W	0	0	0	0	1	0
WL	0	0	0	0	0	2

Accuracy 0.923

Bands + Index-Select class

	S	VW	HP	UA	W
S	2	0	0	0	0
VW	0	2	0	0	0
HP	0	0	4	0	0
UA	0	0	1	1	0
W	0	0	0	0	1

Accuracy 0.909

Lot 2

Bands- All class

	S	VW	HP	UA	W	WL
S	2	0	0	0	0	0
VW	0	1	1	0	0	0
HP	0	0	1	0	0	0
UA	1	0	0	3	0	0
W	0	0	0	0	1	0
WL	0	0	0	0	0	1

Accuracy 0.818

Bands + Index - All class

	S	VW	HP	UA	W	WL
S	2	0	0	0	0	0
VW	0	1	1	0	0	0
HP	0	0	0	0	0	0
UA	1	0	1	3	0	0
W	0	0	0	0	1	0
WL	0	0	0	0	0	1

Accuracy 0.727

Bands + Index-Select class

	S	VW	HP	UA
S	2	0	0	0
VW	0	1	1	0
HP	0	0	0	0
UA	1	0	1	3

Accuracy 0.667

◂ **Fig. 3** Model selection parameters for the classification of diseases and physiological disorders in potato plants of the variety Diacol Capiro. **A** Receiver operation characteristic (ROC) curves and area under the curve (AUC) values. **B** Confusion matrix. Vertical rows, true class; horizontal column, predicted class. S, soil; VW, *Verticillium* wilt; HP, healthy plants; UA, unknown alteration; W, water; WL, waterlogging

from diseased plants with UA and VW according to the RMSEP statistics. GNDVI was found as the index with the highest predictive power, followed by indices NDVI, SAVI, EVI, MSAVI, and VARI, respectively (Table 2).

Detection of potato diseases and physiological disorders using machine learning and remote sensing

Table 3 shows the results of the ability of RF to prioritize the importance of variables (bands and indices) and their discriminating ability of class associated with different physiopathologies after an internal optimization process (number of trees, number and depth of nodes, hyperparameter alpha and significance). It was determined that the RF had an outstanding performance for this research based on the test statistics evaluated (Table 3).

The weight of the predictive variables changed regarding each class and plot evaluated. In plot 1, it was found that for VW, WL, and HP, the green and NIR bands and the NDVI index provide the greatest importance in the classifier. For UA, it was found that the green and blue bands, besides the NDVI and GNDVI indices, have relevance in the differentiation of this class. The predictive variables in plot 2 did not show contrasting values between them regarding their importance (Fig. 2).

Concerning the prediction capacity, it was found that the evaluated alterations showed AUC values close to 1, indicating good sensitivity and specificity of the model. It was possible to predict classes S, VW, HP, W, and UA with higher values in plot 1 compared to plot 2. This may be highly related to a larger leaf area affected (over 30%) in plot 1. It was also found that the combination of bands and indices and, to a greater extent, the reduction of the classes improved the model's ability to predict, based on a better performance of the metrics (Fig. 3A). These results were corroborated by the confusion matrix, in which classifications for plot 2 showed OA values below 60%, indicating high error rates. This is contrary to plot 1 where OA values were greater than 74%. The reduction of classes improved the predictive capacity of the algorithm, achieving an OA greater than 87% (Fig. 3B).

The classifier with the best results was the one that used the spectral bands as predictive variables and considered the following classes (S, VW, UA, W, and HP); the classifier with the worst results considered all classes using the spectral bands and the spectral indices as predictive variables (Fig. 3 A and B). To corroborate the results found with the OA and ROC-AUC metrics, the accuracy and kappa index parameters showed the same behavior; they also indicate that the classification in plot 2 does not represent a good estimate of real phytosanitary status under field conditions (Table 3 and Figs. 4–6).

Figures 4, 5, and 6 show the visualization of the classification of the previously mentioned combinations in the evaluated plots. In each of the evaluated models (Table 1, Figs. 4, 5, and 6), it was found that 100% of the classes associated with VW in plot 1 were discriminated correctly, whereas for plot 2, an underestimation was presented (values between 50 and 100%). For WL, 100% of classes were classified correctly for the three models in the two plots evaluated. UA showed contrasting results, plot 1 showed an underestimation, resulting in only 50% of classes being correctly identified, while in plot 2, the result was an overestimation, with increases of 300% (Figs. 4, 5, and 6).

Discussion

UA was important in the evaluated plots and the described symptoms did not match the diseases or disorders reported in potato crops (Stevenson et al. 2002; Torres 2002). For this reason, this symptomatology was called unknown alteration. On the other hand, plants showing vascular wilt from which *Verticillium* sp. was isolated matched the reports of the disease in potato plants (Krikun and Orion 1979; Stevenson et al. 2002; Torres 2002; Johnson and Dung 2010; Wheeler and Johnson 2016). Regarding the third physiopathology, its

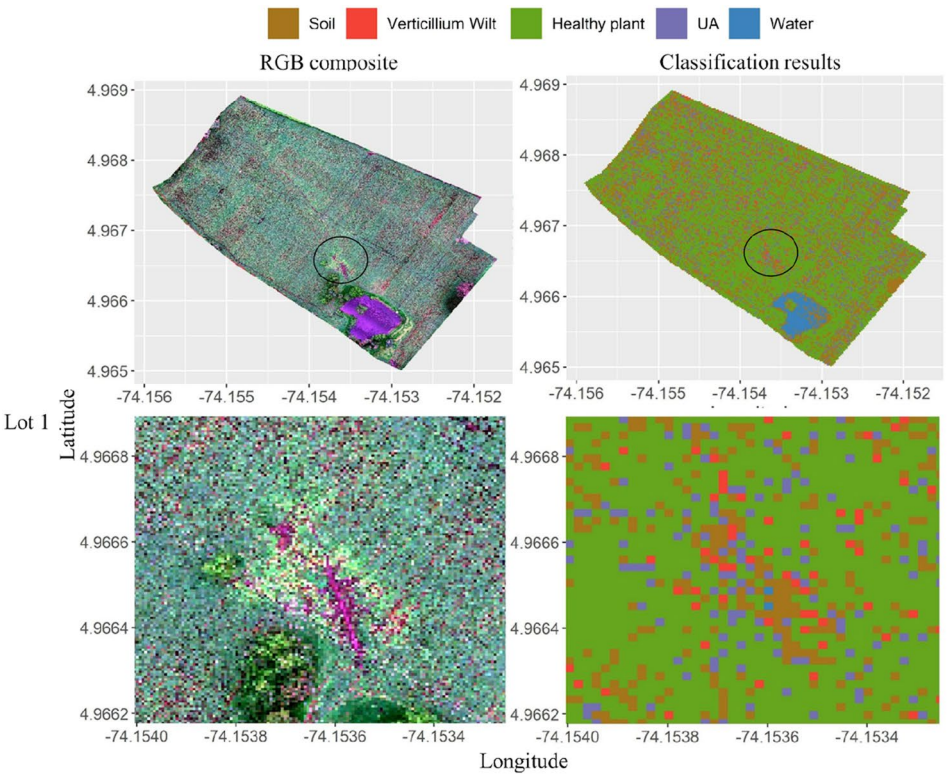

Class	Soil	Verticillium wilt	Healthy plants	UA	Water
Field condition (number)	22	25	45	12	10
Classification (%)	100	100	100	50	100

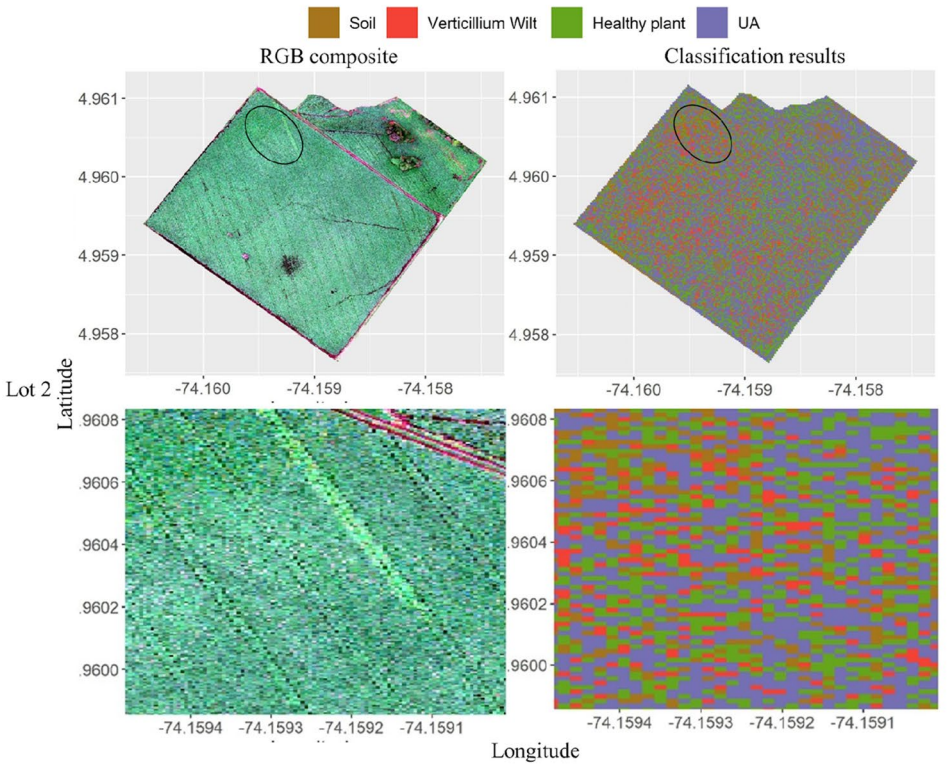

Class	Soil	Verticillium wilt	Healthy plants	UA
Real under field condition (%)	20	15	50	20
Classification (%)	100	50	100	60

◂**Fig. 4** Classification of diseases and physiological disorders in potato plants of the variety Diacol Capiro under field conditions using random forest with spectral bands + vegetation index and selected classes. UA: unknown alteration

expression in plants was associated with waterlogging stress (Orsák et al. 2020). The fourth disease was associated with late blight caused by *P. infestans* (Fry et al. 1993). To manage this disease, fungicide applications are carried out during the crop cycle (Silva et al. 2010), which possibly explains the low incidence and leaf area affected (severity) found in the evaluated plots.

The vegetation indices used in this research showed contrasting results since it was only possible to have a high discriminative capacity between healthy plants and those with UA and VW with the use of GNDVI and NDVI. The evaluated indices were a tool that allows early detection of stress sources in multiple production systems, including potatoes. However, they have some limitations especially associated with sensitivity and specificity, when used under field conditions (Yang et al. 2007; Naidu et al. 2009; Dash et al. 2017; Couture et al. 2018; Duarte-Carvajalino et al. 2018; Polder et al. 2019).

The RF algorithm, a machine learning tool, was used in this study as an alternative that allowed a suitable approximation to the indirect detection of different disorders and sanitary problems in potato crops under field conditions, considering spectral bands acquired using the multispectral cameras attached to drones and the calculated vegetation indices (Figs. 4–6). The RF algorithm has multiple advantages over other machine learning tools, given its simplicity in terms of the number of parameters to be optimized (Svetnik et al. 2003; Pal 2005).

We included the spectral indices as additional training/testing data to improve the prediction capacity of the algorithm used in this research. The classifier's results were improved by the spectral classes, which is the opposite of what the literature states (Fletcher 2016).

The stresses evaluated in our study are a response to different biotic or abiotic factors, but the visible expression of these alterations coincides in several of them. In our case, they can be grouped instead into the normal green color of the plant (WL, VW), tissue necrosis (LB, VW), and turgor changes (VW). The changes found in the plants were reflected in specific informative bands and, therefore, in the indices evaluated. In this sense, NDVI showed good discrimination capacity for UA according to GLM, but this was not reflected in the variable prioritization with RF algorithm. The GNDVI showed a high differentiation capacity of VW, coinciding with the GLM and RF algorithm. These results indicate that the most informative spectral bands for the detection of alterations in potatoes are green, red, and near infrared. These bands have been associated with the ability to detect changes in color, structure density, and biochemical condition of leaves (Yang et al. 2007; Naidu et al. 2009; Lowe et al. 2017). In addition, the NDVI was successful in detecting symptoms of advanced stages of VW such as foliar chlorosis, leaf, wilting, and defoliation (Calderón et al. 2013), which coincides with the low discrimination capacity found in plot 2 given the low incidence and severity displayed by VW.

Based on the GML, kappa index, and RF algorithm, our results showed a moderate to good discrimination capacity for VW and UA. Nevertheless, the more diverse symptoms profile in VW may explain the higher variation in the discrimination power among the evaluated indices (Table 2). In contrast, events of UA, with less variation in the visual symptoms, were well discriminated more often according to the kappa index. In our study, the variation observed among indices and a disease or disorder in potato crops could be related to the level of variation in the expressed symptoms. This may involve one or more physiological responses reflected in the detected spectral responses (Lowe et al. 2017). Additionally, the degree of severity was a highly determining factor of the discriminant capacity of the evaluated methods. This explains the obtained results in plot 2, where the severity of all diseases and disorders was less than 10% of leaf area affected. Moreover, it was not possible to discriminate the class associated with late blight (LB) despite previous reports of success under low severity levels (Franceschini et al. 2019).

Using data from multispectral sensors attached to UAVs showed a great potential in the identification and

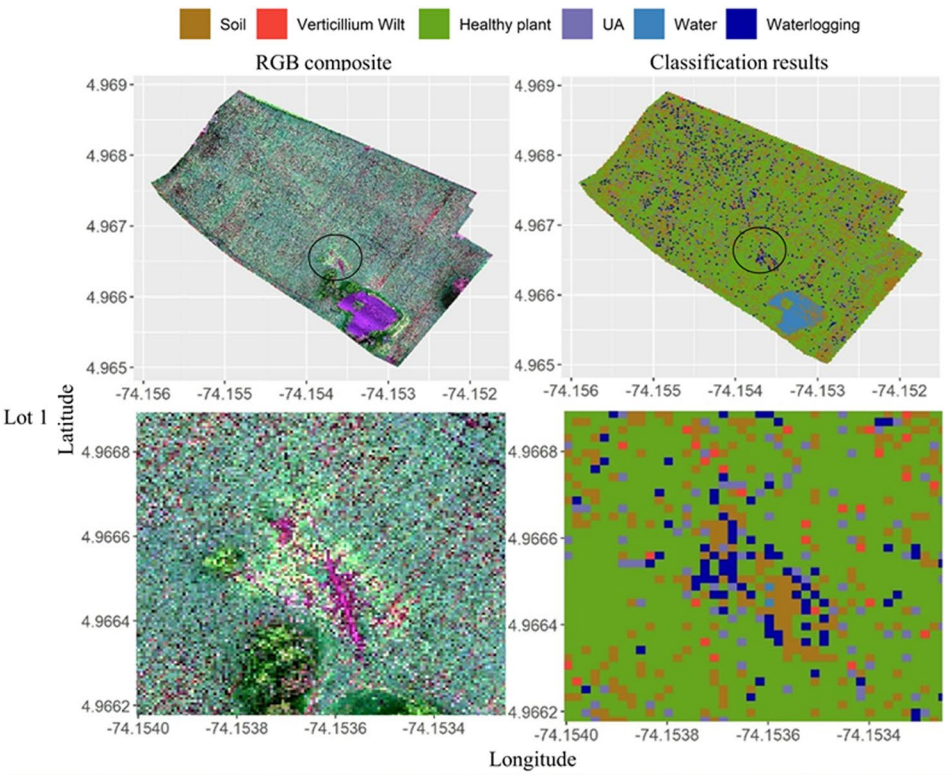

Class	Soil	Verticillium wilt	Healthy plant	UA	Water	Waterlogging
Field condition (number)	22	25	45	12	10	15
Classification (%)	100	100	100	50	100	100

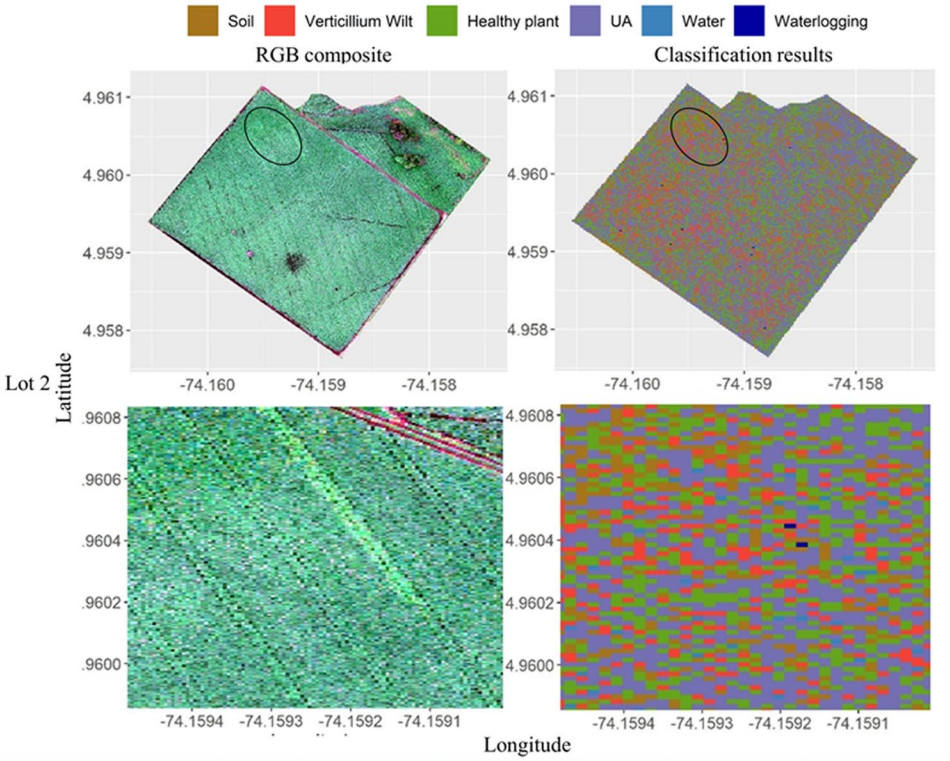

Class	Soil	Verticillium wilt	Healthy plant	UA	Water	Waterlogging
Field condition (number)	20	20	50	20	10	15
Classification (%)	100	50	100	200	100	100

◂ **Fig. 5** Classification of diseases and physiological disorders in potato plants of the variety Diacol Capiro under field conditions using random forest with bands + vegetation index including all classes.UA: unknown alteration

discrimination of different diseases and physiological disorders in potato crops, becoming commercially important for the identification of sources of stress associated with biotic and abiotic factors (Fang and Ramasamy 2015; Lowe et al. 2017; Mahlein et al. 2018). When attached to UAVs, these sensors have advantages over the use of aircrafts or satellites for the same purposes, since they can provide a higher spatial resolution, operate locally, and manage to penetrate inaccessible areas (Dash et al. 2017). This allows their commercial use in potato production systems as it has been demonstrated before (Gibson-Poole et al. 2017; Franceschini et al. 2019; Li et al. 2019).

The limitations found in our study were associated with (i) unbalanced classes and (ii) classes that could not be classified (late blight). Our explanation is focused on the fact that our analysis was performed under field conditions in commercial crops, with phytosanitary problems presented in a differential way in terms of disease or disorder level and depending on several factors (e.g., farmer considerations and tools for diseases management, among others). These conditions generated unbalanced classes that can significantly affect the classification (del Río et al. 2014), a phenomenon observed in plot 2 with a greater impact. In contrast, the classification capacity in plot 1 improved when we changed the prediction rule for another with majority vote incorporating artificial class weights into the RF classifier (Liaw and Wiener 2002; del Río et al. 2014). Another source of variation was generated as a consequence of the number of samples (n) and sampling units that were reduced to achieve a "practical sampling for the farmers." However, the results indicated the need to increase the n and use a homogeneous sampling unit to obtain the "optimal samples" in order to improve the performance of the classifier (Mellor et al. 2015).

The results of this research are a contribution to the visual recognition assisted by sensors of diseases and disorders such as VW and UA that are difficult to identify and discriminate in the field even at advanced stages. However, limitations associated with the detection of other plant alterations and high variation at the plot level were observed due to multiple factors such as temporality, spatial resolution, and the limited training data for the models (Immitzer et al. 2012). The small amount of data for calibration and evaluation leads to increases in errors and, therefore, decreases in the prediction capacity of the GLM (Vidoni 2003). This phenomenon has also been reported as limiting in the supervised classification using the RF algorithm, where it causes confusion in the model (Millard and Richardson 2015).

Despite these constraints, monitoring and image capture are recommended throughout the crop cycle since they can provide data on symptomatic variability that improves the differentiation between classes (Watts et al. 2011). Based on our results, we may consider that increasing the spatial resolution could increase the possibility of differentiating characteristic lesions or symptoms of each one of the alterations. This along with a greater number of field evaluation points per unit area, more assessments during the crop cycle, and additional vegetation indices considered can enhance the predictive capacity of the algorithm (Immitzer et al. 2012). For subsequent studies, we also recommend the use of other algorithms to evaluate and compare their predictive capacity.

Spectral cameras attached to UAVs, sampling in the field, and the correct machine learning analysis are tools with a high potential application in the detection of diseases and physiological disorders in commercial potato production systems. From our study, we can conclude that in order to improve the capacity of a predictive model based on monitoring and image capture for more than one plant disease or disorder taking place under commercial conditions, it is highly recommended to increase the spatial resolution, use a high number of evaluation points per unit area, and perform more than one assessment during the crop cycle.

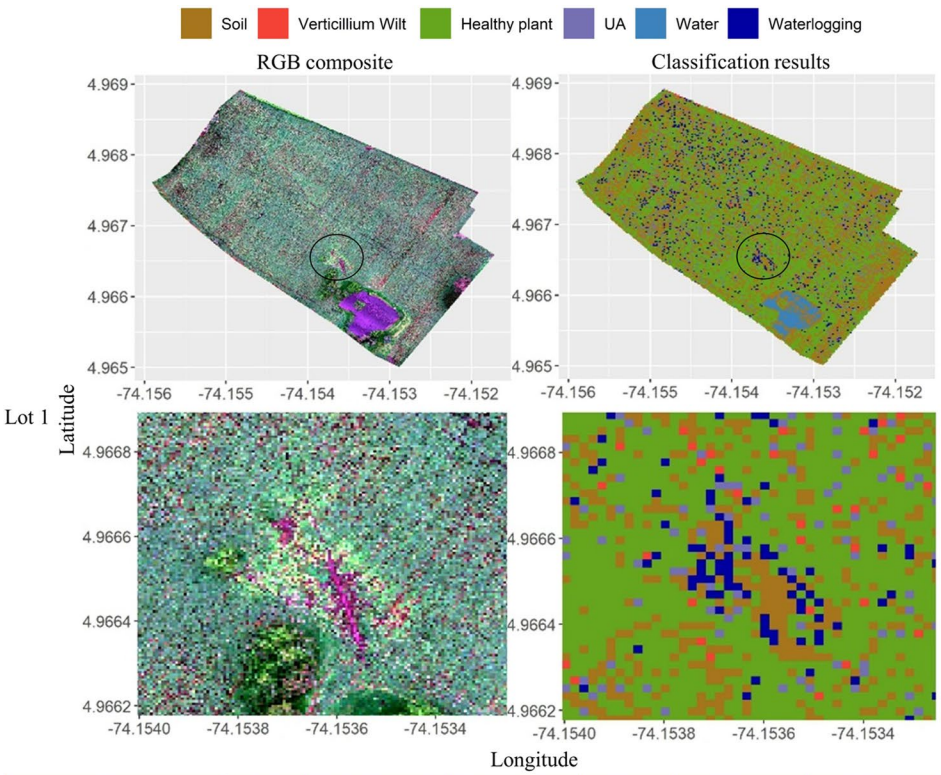

Class	Soil	Verticillium wilt	Healthy plant	UA	Water	Waterlogging
Field condition (number)	22	25	45	12	10	15
Classification (%)	100	100	100	50	100	100

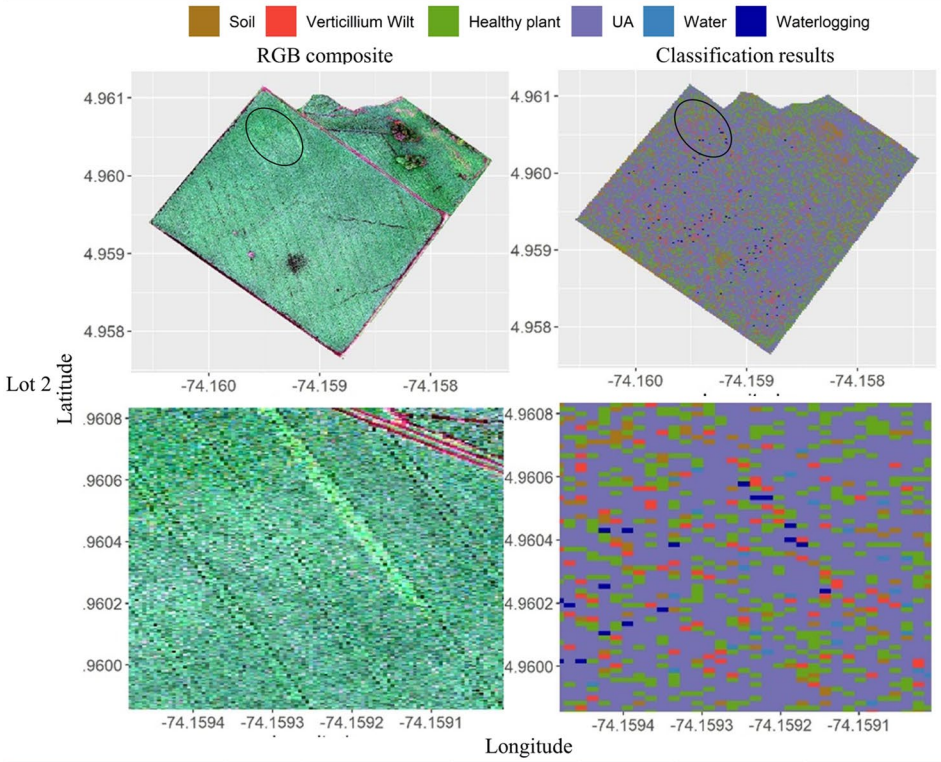

Class	Soil	Verticillium wilt	Healthy plant	UA	Water	Waterlogging
Field condition (number)	20	15	50	20	10	15
Classification (%)	100	100	100	300	100	100

◂**Fig. 6** Classification of diseases and physiological disorders in potato plants of the variety Diacol Capiro under field conditions using random forest with spectral bands and all classes. UA: unknown alteration

Supplementary Information The online version contains supplementary material available at https://doi.org/10.1007/s40858-021-00460-2.

Acknowledgements The authors would like to thank the "Semillero de Investigación en Geomática Aplicada" for the loan of the drone and the spectral camera for field work. We would also like to thank several potato farmers and Sumiagro (™) for their valuable information and support during this research. In addition, we want to thank Professor Ivan Alberto Lizarazo Salcedo of the Universidad Nacional for his valuable help in the data analysis.

Author contribution Conceptualization: JGRG, SGC. Data curation: JGRG, WALR. Formal analysis: JGRG, WALR. Investigation: JGRG, SGC, WALR. Methodology: JGRG, WALR. Software: JGRG, WALR. Writing, original draft preparation: JGRG, WALR. Writing, review and editing: JGRG. Supervision: JGRG, CL. All authors have read and agreed to the published version of the manuscript.

Data availability The data sets generated during and/or analyzed during the current study are available from the corresponding author on reasonable request.

Declarations

Conflict of interest The authors declare no competing interests.

References

Barnett HL, Hunter BB (1972) Illustrated genera of imperfect fungi. Burgess Publishing Company, Minnesota E.U

Bekkar M, Djemaa HK, Alitouche TA (2013) Evaluation measures for models assessment over imbalanced data sets. Journal of Information Engineering and Applications 3:27–38–38

Breiman L (1996) Bagging predictors. Mach Learn 24:123–140. https://doi.org/10.1007/BF00058655

Buriticá-Cespedes P (1999) Directorio de patógenos y enfermedades de las plantas de importancia económica en Colombia, Instituto Colombiano Agropecuario (ICA). Universidad Nacional de Colombia, Medellín Colombia

Calderón R, Navas-Cortés JA, Lucena C, Zarco-Tejada PJ (2013) High-resolution airborne hyperspectral and thermal imagery for early detection of Verticillium wilt of olive using fluorescence, temperature and narrowband spectral indices. Remote Sensing of Environment 139:231–245. https://doi.org/10.1016/j.rse.2013.07.031

Céspedes MC, Cárdenas ME, Vargas AM, Rojas A, Morales JG, Jiménez P, Bernal AJ, Restrepo S (2013) Physiological and molecular characterization of *Phytophthora infestans* isolates from the Central Colombian Andean Region. Revista Iberoamericana de Micología 30:81–87

Cochran W (1977) Sampling techniques, 3rd edn. Wiley, New York

Cortes C, Mohri M (2003) AUC optimization vs. error rate minimization. In: Proceedings of the 16th International Conference on Neural Information Processing Systems. MIT Press, Whistler, British Columbia, Canada, pp 313–320

Couture JJ, Singh A, Charkowski AO, Groves RL, Gray SM, Bethke PC, Townsend PA (2018) Integrating spectroscopy with potato disease management. Plant Disease 102:2233–2240

Dash JP, Watt MS, Pearse GD, Heaphy M, Dungey HS (2017) Assessing very high resolution UAV imagery for monitoring forest health during a simulated disease outbreak. ISPRS Journal of Photogrammetry and Remote Sensing 131:1–14

del Río S, López V, Benítez JM, Herrera F (2014) On the use of MapReduce for imbalanced big data using Random Forest. Information Sciences 285:112–137. https://doi.org/10.1016/j.ins.2014.03.043

Duarte-Carvajalino JM, Alzate DF, Ramirez AA, Santa-Sepulveda JD, Fajardo-Rojas AE, Soto-Suárez M (2018) Evaluating late blight severity in potato crops using unmanned aerial vehicles and machine learning algorithms. Remote Sensing 10:1513

Erwin DC, Ribeiro OK (1996) *Phytophthora* diseases worldwide, Edición, illustrated. American Phytopathological Society, St. Paul

Fang Y, Ramasamy RP (2015) Current and prospective methods for plant disease detection. Biosensors 5:537

Fletcher RS (2016) Using vegetation indices as input into random forest for soybean and weed classification. American Journal of Plant Sciences 7:720–726

Fox J, Weisberg S, Price B, et al (2020) car: Companion to Applied Regression. Version 3.0-10URL. https://CRAN.R-project.org/package=car

Franceschini MHD, Bartholomeus H, van Apeldoorn DF, Suomalainen J, Kooistra L (2019) Feasibility of unmanned aerial vehicle optical imagery for early detection and severity assessment of late blight in potato. Remote Sensing 11:224

Fry W, Goodwin S, Dyer A, Matuszak JM, Drenth A, Tooley PW, Sujkowski LS, Koh YJ, Cohe BA, Spielman LJ, Deahl KL, InglisSandlan DAKP (1993) Historical and recent migrations of *Phytophthora infestans*: chronology, pathways, and implications. Plant Disease 77:653–661

Gibson-Poole S, Humphris S, Toth I, Hamilton A (2017) Identification of the onset of disease within a potato crop using a UAV equipped with un-modified and modified commercial off-the-shelf digital cameras. Advances in Animal Biosciences 8:812–816

Hasmadi M, Pakhriazad H, Shahrin M (2009) Evaluating supervised and unsupervised techniques for land cover mapping using remote sensing data. Geografia-Malaysian Journal of Society and Space 5:1–10

Hijman RJ (2016) Package 'raster'

Immitzer M, Atzberger C, Koukal T (2012) Tree species classification with random forest using very high spatial resolution 8-Band WorldView-2 Satellite Data. Remote Sensing 4:2661–2693

Johnson DA, Dung J (2010) Verticillium wilt of potato – the pathogen, disease and management. Canadian Journal of Plant Pathology 32:58–67

Krikun J, Orion D (1979) Verticillium wilt of potato: Importance and control. Phytoparasitica 7:107

Kuhn M, Wing J, Weston S, Williams A, Keefer C, Engelhardt A, Cooper T, Mayer Z, Kenkel B, R Core Team, Benesty M, Lescarbeau R, Ziem A, Scrucca L, Tang Y, Candan C, Hunt T (2020) caret: classification and regression training

Henao-Rojas JC, Rosero-Alpala MG, Ortiz-Muñoz C, et al (2021) Machine Learning Applications and Optimization of Clustering Methods Improve the Selection of Descriptors in Blackberry Germplasm Banks. Plants (Basel) 10. https://doi.org/10.3390/plants10020247

Li B, Xu X, Han J, Zhang L, Bian C, Jin L, Liu J (2019) The estimation of crop emergence in potatoes by UAV RGB imagery. Plant Methods 15:15

Liaw A, Wiener M (2002) Classification and regression by randomForest. R News 2:18–22
Liaw A, Wiener M (2018) randomForest: Breiman and Cutler's random forests for classification and regression. Version 4.6–14URL https://CRAN.R-project.org/package=randomForest
Lowe A, Harrison N, French AP (2017) Hyperspectral image analysis techniques for the detection and classification of the early onset of plant disease and stress. Plant Methods 13:1–12
Mahlein A-K, Kuska MT, Behmann J, Polder G, Walter A (2018) Hyperspectral sensors and imaging technologies in Phytopathology: State of the art. Annual Review of Phytopathology 56:535–558
Mahlein A-K, Kuska MT, Thomas S, Bohnenkamp D, Alisaac E, Behmann J (2017) Plant disease detection by hyperspectral imaging: from the lab to the field. Advances in Animal Biosciences 8:238–243
Martinelli F, Scalenghe R, Davino S, Panno S, Scuderi G, Ruisi P, Villa P, Stroppiana D, Boschetti M, Goulart LR, Davis CE, Dandekar AM (2015) Advanced methods of plant disease detection. A review. Agronomy for Sustainable Development 35:1–25
Mellor A, Boukir S, Haywood A, Jones S (2015) Exploring issues of training data imbalance and mislabelling on random forest performance for large area land cover classification using the ensemble margin. ISPRS. Journal of Photogrammetry and Remote Sensing 105:155–168. https://doi.org/10.1016/j.isprsjprs.2015.03.014
Millard K, Richardson M (2015) On the importance of training data sample selection in random forest image classification: a case study in peatland ecosystem mapping. Remote Sensing 7:8489–8515
Miller SA, Beed FD, Harmon CL (2009) Plant disease diagnostic capabilities and networks. Annual Review of Phytopathology 47:15–38
Mondal P (2011) Quantifying surface gradients with a 2-band enhanced vegetation index (EVI2). Ecological Indicators 11:918–924
Mueller A, Guido S (2016) Introduction to machine learning with Python: a guide for data scientists, Dawn Sachanafelt. O'Reilly Media, Sebastopol, CA
Naidu RA, Perry EM, Pierce FJ, Mekuria T (2009) The potential of spectral reflectance technique for the detection of Grapevine leafroll-associated virus-3 in two red-berried wine grape cultivars. Computers and Electronics in Agriculture 66:38–45
Nieto L (1988) La madurez prematura de la papa causada por *Verticillium* spp. en Colombia. Revista ICA 4:334–340
Oerke E-C, Steiner U, Dehne H-W, Lindenthal M (2006) Thermal imaging of cucumber leaves affected by downy mildew and environmental conditions. Journal of Experimental Botany 57:2121–2132
Orsák M, Kotíková Z, Hnilička F, Lachman J, Stanovič R (2020) Effect of drought and waterlogging on hydrophilic antioxidants and their activity in potato tubers. Plant, Soil and Environment 66:128–134
Pal M (2005) Random forest classifier for remote sensing classification. International Journal of Remote Sensing 26:217–222
Paluszynska A, Biecek P, Jiangaut Y, cre (2019) randomForestExplainer: Explaining and Visualizing Random Forests in Terms of Variable Importance. Version 0.10.0. https://CRAN.Rproject.org/package=randomForestExplainer
Polder G, Blok PM, de Villiers HAC, van der Wolf JM, Kamp J (2019) Potato virus Y detection in seed potatoes using deep learning on hyperspectral images. Frontiers in Plant Science 10:1–13
Qi J, Chehbouni A, Huete AR, Kerr YH, Sorooshian S (1994) A modified soil adjusted vegetation index. Remote Sensing of Environment 48:119–126
R Development Core Team (2020) R: the R project for statistical computing. In: R Foundation for Statistical Computing, Vienna, Austria. https://www.r-project.org/. Accessed 1 Jun 2020
Ramirez-Gil JG, Garcia C, Navas J, Leon J, Góme-Caro S. 2019. Implicaciones epidemológicas y económicas de Verticillium sp., en una región productora de papa en Cundinamarca, in: XXXIV CONGRESO COLOMBIANO DE FITOPOPATOLOGIA Y CIENCIAS AFINES MEMORIAS. Presented at the XXXIV CONGRESO COLOMBIANO DE FITOPOPATOLOGIA Y CIENCIAS AFINES MEMORIAS, Fitopatologia Colombiana, Cudinamarca Colombia, pp. 206–207
Ramirez-Gil J, Navas J, Góme-Caro S (2019b) Epidemiología e importancia económica de una alteración de origen desconocido en papa en la sabana occidente de Cundinamarca. In: XXXIV CONGRESO COLOMBIANO DE FITOPOPATOLOGIA Y CIENCIAS AFINES MEMORIAS. Fitopatologia Colombiana, Cudinamarca Colombia, pp 205–205
Ramírez-Gil JG, Morales-Osorio JG (2018) Microbial dynamics in the soil and presence of the avocado wilt complex in plots cultivated with avocado cv. Hass under ENSO phenomena (El Niño – La Niña). Scientia Horticulturae 240:273–280
Ristaino JB (2002) Tracking historic migrations of the Irish potato famine pathogen, *Phytophthora infestans*. Microbes and Infection 4:1369–1377
Robin X, Turck N, Hainard A, et al (2021) pROC: Display and Analyze ROC Curves. Version 1.17.0.1. https://CRAN.R-project.org/package=pROC
Sarparast M (2018) LSRS: land surface remote sensing. Version 0.2.0URL https://CRAN.R-project.org/package=LSRS
Seifert K, Morgan-Jones G, Gams W, Kendrick B (2011) The genera of Hyphomycetes. CBS-KNAW Fungal Biodiversity Centre, Utrecht, Netherlands
Silva B, Cotes JM, Marín M (2010) Population structure of *Phytophthora infestans* in potato crops from Antioquia, Boyaca, Cundinamarca, and Norte de Santander (Colombia). Agronomía Colombiana 28:375–382
Stevenson W, Loria R, Frank G, Weingartner D (2002) Compendium of Potato Diseases, W.R. Stevenson , R. Loria, G.D. Franc and D.P. Weingartner. American Phytopathological Society Press, St. Paul USA
Svetnik V, Liaw A, Tong C, Culberson JC, Sheridan RP, Feuston BP (2003) Random forest: a classification and regression tool for compound classification and QSAR modeling. Journal for Chemical Information and Computer Scientists 43:1947–1958
Torres H (2002) Manual de las enfermedades más importantes de la papa en el Perú, Centro internacional de la papa. Centro internacional de la papa., Lima, Peru
Tu Y-H, Phinn S, Johansen K et al (2020) Optimising drone flight planning for measuring horticultural tree crop structure. ISPRS Journal of Photogrammetry and Remote Sensing 160:83–96. https://doi.org/10.1016/j.isprsjprs.2019.12.006
Vidoni P (2003) Prediction and calibration in generalized linear models. Annals of the Institute of Statistical Mathematics 55:169–185
Viera AJ, Garrett JM (2005) Understanding interobserver agreement: the kappa statistic. Family Medicine 37:360–363
Watts JD, Powell SL, Lawrence RL, Hilker T (2011) Improved classification of conservation tillage adoption using high temporal and synthetic satellite imagery. Remote Sensing of Environment 115:66–75
Wheeler DL, Johnson DA (2016) *Verticillium dahliae* infects, alters plant biomass, and produces inoculum on rotation crops. Phytopathology 106:602–613
Yang C-M, Cheng C-H, Chen R-K (2007) Changes in spectral characteristics of rice canopy infested with brown planthopper and leaffolder. Crop Science 47:329–335